Achievable Performance and Effective Interrogator Design for SAW RFID Sensor Tags

Abstract

For many NASA missions, remote sensing is a critical application that supports activities such as environmental monitoring, planetary science, structural shape and health monitoring, non-destructive evaluation, etc. The utility of the remote sensing devices themselves is greatly increased if they are "passive" – that is, they do not require any on-board power supply such as batteries – and if they can be identified uniquely during the sensor interrogation process. Additional passive sensor characteristics that enable greater utilization in space applications are small size and weight, long read ranges with low interrogator power, ruggedness, and operability in extreme environments (vacuum, extreme high/low temperature, high radiation, etc.) In this paper, we consider one very promising passive sensor technology, called *surface acoustic wave* (SAW) *radio-frequency identification* (RFID), that satisfies all of these criteria.

Although SAW RFID tags have great potential for use in numerous space-based remote sensing applications, the limited collision resolution capability of current generation tags limits the performance in a cluttered sensing environment. That is, as more SAW-based sensors are added to the environment, numerous tag responses are superimposed at the receiver and decoding all or even a subset of the telemetry becomes increasingly difficult. Background clutter generated by reflectors other than the sensors themselves is also a problem, as is multipath interference and signal distortion, but the limiting factor in many remote sensing applications can be expected to be tag mutual interference. This problem may be greatly mitigated by proper design of the SAW tag waveform, but that remains an open research problem, and in the meantime, several other related questions remain to be answered including:

- What are the fundamental relationships between tag parameters such as bit-rate, time-bandwidth-product, SNR, and achievable collision resolution?
- What are the differences in optimal or near-optimal interrogator designs between noise-limited environments and interference-limited environments?
- What are the performance characteristics of different interrogator designs in term of parameters such as transmitter power level, range, and number of interfering tags?

In this paper, we present the results of a research effort aimed at providing at least partial answers to all of these questions.

1. Introduction

For many NASA missions, remote sensing is a critical application that supports activities such as environmental monitoring, planetary science, structural shape and health monitoring, non-destructive evaluation, etc. The utility of the remote sensing devices themselves is greatly increased if they are "passive" – that is, they do not require any on-board power supply such as batteries – and if they can be identified uniquely during the sensor interrogation process. Additional passive sensor characteristics that enable greater utilization in space applications are small size and weight, long read ranges with low interrogator power, ruggedness, and operability in extreme environments (vacuum, extreme high/low temperature, high radiation, etc.) In this proposal, we consider one very promising passive sensor technology, called *surface acoustic wave* (SAW) *radio-frequency identification* (RFID), that satisfies all of these criteria.

In general, RFID is a method of identifying items using radio waves to interrogate "tags" encoded with a unique identifier that are affixed to the items of interest. In the case of passive tags, only the interrogator, which transmits power to the tags in the form of radio-frequency electromagnetic radiation, requires access to a power supply. Passive RFID technologies are used today in many applications, including asset tracking and management, security and access control, and remote sensing. To date, most of the development and application in RFID technology has focused on either asset/inventory tracking and control or security and access control because these are the largest commercial application areas. Recently, however, there has been growing interest in using passive RFID technology for remote sensing applications, and SAW devices are at the forefront of RFID sensing technology development [1-6]. In addition, a recent breakthrough [7] has dramatically increased the data capacity of SAW-based RFID thereby increasing its usefulness as a platform for remote sensing systems.

Although SAW RFID tags have great potential for use in numerous space-based remote sensing applications, the limited collision resolution capability of current generation tags limits the performance in a cluttered sensing environment. That is, as more SAW-based sensors are added to the environment, numerous tag responses are superimposed at the receiver and decoding all or even a subset of the telemetry becomes increasingly difficult. Background clutter generated by reflectors other than the sensors themselves is also a problem, as is multipath interference and signal distortion, but the limiting factor in many remote sensing applications can be expected to be tag mutual interference.

This problem can be greatly mitigated by proper design of the SAW tag waveform, even within the constraints imposed by the physical characteristics of SAW devices. In particular, results from coding theory and multi-user communication and information theory can be applied to develop tag encoding and decoding schemes that are superior to the conventional ad-hoc spread-spectrum techniques that are currently utilized [14, 15] and to derive performance bounds that can be utilized as benchmarks for design and performance evaluation. Such new, improved tag encoding and decoding techniques are currently under investigation at NASA JSC, but finding the best approach remains an open research problem. In the meantime, several other related questions remain to be answered including:

- What are the fundamental relationships between tag parameters such as bit-rate, time-bandwidth-product, SNR, and achievable collision resolution?
- What are the differences in optimal or near-optimal interrogator designs between noise-limited environments and interference-limited environments?

- What are the performance characteristics of different interrogator designs in term of parameters such as transmitter power level, range, and number of interfering tags?

Answers to all of these questions are provided in this paper, which is organized as follows. Section 2 presents some background information on SAW RFID tags. A number of useful theoretical results are presented and discussed in Section 3. In Section 4, a useful model for the analysis of large populations of SAW tags is introduced and expressions for optimal interrogator design and performance are derived. The results of both numerical and simulated interrogator performance evaluations are presented in Section 5. A summary of the results presented in the paper along with some concluding remarks are presented in Section 6. Finally, some details regarding the model adopted for SAW tag analysis in Section 4 are presented in an Appendix.

2. Background on SAW tags

SAW RFID technology differs from more conventional integrated-circuit (IC) based RFID technology in many significant ways. For example, SAW RFID tags do not need to rectify incident electromagnetic power arriving at the tag. Instead, they modulate and re-radiate the interrogation signal directly using a series of reflectors printed on the surface of the device. The design and operation of a typical SAW RFID tag is illustrated in Figure 1.

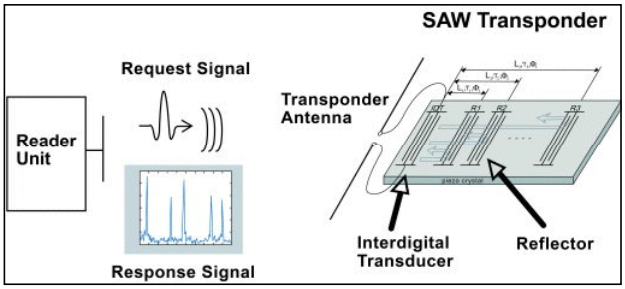

Figure 1. Design and operation of a typical SAW RFID tag.

The principle benefit of this approach is that SAW RFID tags are capable of operating at much lower interrogator transmit power, and/or are capable of much greater range for a given transmit power than IC-based tags [Hartmann, et al.]. In addition, SAW RFID tags have the capability to incorporate certain types of sensor telemetry along with the identification information. For example, the impulse response of a SAW RFID tag is highly sensitive to temperature. The temperature of the tag can be estimated directly by using a correlation operation to measure the time dilation (or contraction) of the impulse response. Finally, SAW RFID tags are very robust and can tolerate extreme conditions that would render IC-based tags inoperable. For example, they can withstand temperatures from cryogenic to over 310° C, they are inherently immune to ionizing radiation, and they have survived shock levels exceeding 1000 G.

The temperature of a SAW RFID tag can be estimated by direct measurement of the time dilation (or contraction) of the tag impulse response. In particular, measurement of the time dilation of the impulse response at an arbitrary temperature relative to the response at a known reference temperature (usually 0° C) constitutes an observation of the *temperature coefficient of delay* (TCD) for the tag at its current temperature. Here, the term TCD refers to the mathematical function of temperature that quantifies the relationship between the relative time dilation of the tag response and the temperature of the tag, with respect to a fixed reference temperature. Although the TCD can theoretically be determined from the piezo-electric properties of the

crystalline material used to manufacture the tag, it is more common (and probably more accurate) to estimate it experimentally.

As an example, consider the waveform presented in Figure 2 below. This waveform represents the magnitude of a normalized version of the impulse response from a SAW RFID tag at a temperature of -73º C. The tag illustrated here is an example of the 40-bit Global SAW tag manufactured by RF SAW, Inc. [Hartmann, et al.]. There are a total of 22 pulses of slightly varying amplitude spaced intermittently over approximately a 1.6 μs time period after an initial delay of approximately 1.2 μs. The exact spacing of the pulses, excluding the first and last pulse (which are used for synchronization) along with the phase of each pulse (which is not visible in Figure 2) encodes the 40-bit ID of the individual tag.

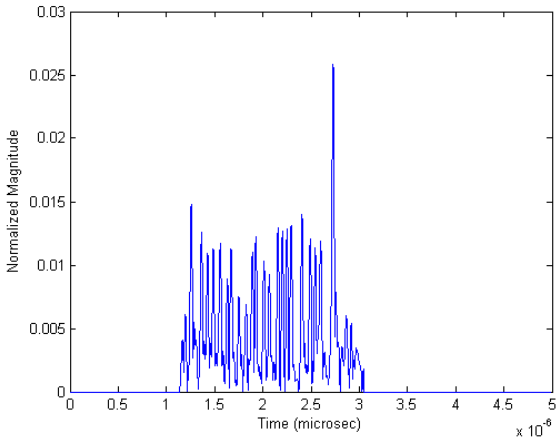

Figure 2. Magnitude of normalized tag impulse response at -73º C.

Finally, Figure 3 shows the magnitude of all 22 pulses in the RFID response waveform at both –73º C (blue) and 21º C (green). It is clear from the figure that the higher temperature waveform has been dilated with respect to the lower temperature waveform. In fact, the dilation factor is approximately 1.0068, which corresponds to a change in dilation factor of approximately 7.2×10^{-5} per degree C. As it turns out, the TCD for these tags is very close to linear over large temperature ranges and 7.2×10^{-5} represents a very good approximation to the slope of the corresponding line in the region from at least -100º C to 100º C.

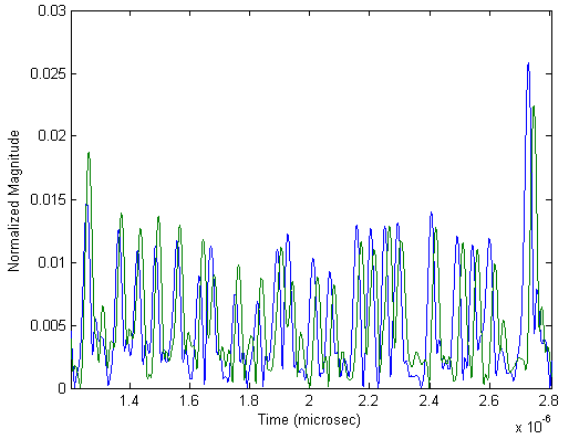

Figure 3. All 22 pulses of SAW tag impulse response magnitude at -73º C (blue) and 21º C (green).

3. Theoretical Results

The results developed in this section are completely general and apply not only to SAW RFID tags but IC-based tags as well. However, since this paper is focused on SAW tags, the discussion has been tailored specifically to those tags.

The RFID interrogation problem is well modeled as a *Gaussian multiple-access channel*. That is, we assume that over some fixed time interval $t \in [0, T]$ following the transmission of an interrogator signal, all of the tags in the environment will respond by transmitting a unique ID signal within a fixed bandwidth $[-B/2, B/2]$ and that the signal received back at the interrogator during this time interval is the superposition of all tag responses plus complex-valued additive white Gaussian noise (AWGN) with power spectral density (PSD) of N_0 watts/Hz. Note that the complex-valued, baseband model adopted here is a reflection of the fact that real-valued signals can be modeled at baseband using complex-valued low-pass equivalent signals [Proakis] with no loss of generality and with less mathematical complexity. Within this very general context, we can determine fairly precisely the relationship between achievable bit-rate per tag (i.e., the number of bits of information communicated by each tag), achievable collision resolution (i.e., how many tags can be simultaneously decoded), time-bandwidth product (*BT* in this case), and signal-to-noise ratio ($SNR = \mathcal{E}_s / N_0$, where $\mathcal{E}_s$ represents the energy received per tag). To do this without expressions or notation becoming cumbersome and somewhat of a distraction, we make the simplifying assumptions that the number *M* of tags in the environment is known, that each tag response is received with identical energy $\mathcal{E}_s$ regardless of its range from the interrogator, that $\mathcal{E}_s$ is also known, and that the bit-rate *R* for all tags is identical. Under these assumptions, *R* is an achievable bit-rate per tag if and only if it satisfies [Cover and Thomas]

$$R \le \frac{BT}{M} \log_2 \left(1 + \frac{M \cdot SNR}{BT} \right). \qquad (1)$$

Equivalently, the maximum total number of tags with fixed bit-rate *R* that can be decoded simultaneously is given by the largest integer satisfying

$$M \le \frac{BT}{R}\log_2\left(1+\frac{M\cdot SNR}{BT}\right). \tag{2}$$

Note that for the simple RFID problem, where the tag ID is the only quantity of interest and no telemetry data (such as temperature) are modulated on the tag response, the bit-rate per tag is just the logarithm, base 2, of the total number of tag IDs (i.e., the size of the *tag constellation*) for which the interrogator is scanning. Note also that modulation of the tag response due to environmental parameters such as temperature, strain, or range represents information encoded in the tag in addition to the tag ID, so the bit-rate per tag increases due to tag modulation just as if the length of the tag ID (equivalently, the size of the tag constellation) increased to represent measured data. This is essentially true whether the environmental modulation is of interest or not, so uncertainty regarding the exact structure of the received tag waveforms due to range, temperature, or other environmental parameters can severely degrade the achievable collision resolution for the tags by effectively increasing the bit-rate. Of course, the amount of information represented by waveform modulation parameters such as time delay or time dilation is limited by the precision with which such parameters can be estimated, which is in turn limited by SNR, so it is difficult to quantify precisely the effective bit-rate per tag in the RFID sensing application. Finally, note that for practical purposes, the number M of tags in the environment is generally much smaller than the size of the tag constellation because interrogators are generally programmed to scan for a relatively large number of possible tags even if it is known that the current environment contains only a subset of those tags.

There are several points of interest regarding Equations (1) and (2). First, the term "R is an achievable bit-rate per tag" means that for a fixed bandwidth of B Hz, *and a sufficiently long time duration T*, there exists a constellation of tag waveforms of size 2^R with time-bandwidth product BT such that if any M waveforms are received at the same time and with the same SNR, all tag IDs can be decoded with arbitrarily low probability of error. The emphasis on sufficiently long time duration is particularly important, since it implies that to achieve a particular bit-rate per tag, it may be necessary to let the tag waveforms become arbitrarily long. Furthermore, since we are fixing the energy received per tag, the average power in the tag waveforms will become arbitrarily small as the waveform duration increases. Hence, one can expect that tags with good collision resolution properties will have relatively long waveforms with low average power.

Secondly, Equation (1) can be rewritten as

$$R \le \frac{BT}{M\ln 2}\ln\left(1+\frac{M\cdot SNR}{BT}\right) \le \frac{SNR}{\ln 2},$$

with equality if and only if $SNR = 0$. Furthermore, for sufficiently small values of the quantity $M\cdot SNR/BT$, we have

$$\frac{BT}{M\ln 2}\ln\left(1+\frac{M\cdot SNR}{BT}\right) \approx \frac{SNR}{\ln 2}.$$

Hence, for all positive values of SNR, the achievable bit-rate per tag is strictly less than $SNR/\ln 2$, and this level of efficiency (measured in terms of the achievable bit-rate per tag per unit of received SNR) can be achieved only if $BT >> M\cdot SNR$. Equivalently, the achievable bit-rate per tag will increase linearly with the SNR at the maximum possible rate of $1/\ln 2$ bits per

tag per unit of SNR increase only as long as the time-bandwidth product of the tags is much greater than the quantity $M \cdot SNR$. Note that this is just another way of saying that the *Shannon limit* for RFID tags is –1.6 dB of received SNR required in order to reliably transmit a single bit per tag over the channel (confer [Proakis] for comparison), and that this level of efficiency can be maintained only as long as $BT >> M \cdot SNR$. This result is probably primarily of theoretical interest since detecting even a single known tag in the environment with an SNR of 100 (20 dB) at close to the Shannon limit of efficiency would require a time-bandwidth product close to 1000.

Finally, the maximum achievable bit-rate given by Equation (1) is probably only achievable using detectors of unreasonable complexity. However, a similar result [Cover and Thomas] shows that a bit-rate of *R* is achievable using more practical *single-user detectors* as long as

$$R \le (BT)\log_2\left(1+\frac{SNR}{BT+[M-1]SNR}\right) \tag{3}$$

or

$$M \le \frac{2^{R/BT}}{2^{R/BT}-1}-\frac{BT}{SNR}. \tag{4}$$

Equations (3) and (4) are probably of much more practical use than Equations (1) and (2) in terms of determining how well a particular tag/interrogator combination is performing relative to a theoretical baseline. Once again, for sufficiently large values of *BT* relative to $M \cdot SNR$, Equation (3) simplifies to

$$R \le \frac{SNR}{\ln 2},$$

so using practical detectors results in no penalty with respect to maximum *efficiently* achievable bit-rate even though there may be a large penalty with respect to true maximum achievable bit-rate.

As an example of what all of this means, suppose we have a constellation of 2^{40} tag waveforms (i.e., 40-bit tag IDs) with bandwidth of 80 MHz and duration 2 μs. If we design an interrogator to look for all 2^{40} possible tag IDs, then assuming that the temperature and range of all the tags are known and each has a received SNR of 20 dB, the true maximum number of tags that can be reliably detected in the environment simultaneously, as given by finding the largest integer satisfying Equation (2), is 12. Using Equation (4) instead to give an estimate of the maximum number of tags that can be detected using practical detectors leads to a bound of only 4. Hence, one can really only expect to be able to detect approximately 4 tags at once from the entire constellation of such tags using an interrogator of reasonable complexity. On the other hand, if we can reduce the number of tags that the interrogator must search for to a mere 2^{20}, then the true maximum number of detectable tags becomes 25 and the number of practically detectable tags becomes 10. Reducing the number of tags in the constellation even further to only 2^{10} gives a true maximum of 65 and a practical maximum of 21. Naturally, attempting to sense any telemetry with the tags in addition to identifying the tag IDs reduces all of these numbers considerably, so it is clear that there is a great benefit to keeping the number of tags that must be recognized by the interrogator to a minimum when attempting to use RFID tags for sensing applications.

4. Interrogator Design

In this section, we consider the problem of interrogating a single SAW RFID tag with a known ID and known range in the presence of multiple interfering tags[1] under the following assumptions:

- The RF propagation environment is well approximated as a simple delay channel with geometric power-decay constant $\alpha \geq 2$.
- The tag of interest is assumed to be known but drawn initially as a random sample from a population of independent, identically distributed (iid) tag ID waveforms with known second-order properties. It is also assumed that any deterministic differential delay between the response of the tag of interest and the interfering tags is know and explicitly represented.
- The interfering tag ID waveforms are unknown but well approximated as iid random samples from a probability distribution of tag ID waveforms with known second-order properties, which may or may not be the same as the second-order properties of the tag of interest.
- The ranges of the interfering tags are unknown but well approximated as independent, identically distributed realizations of a random variable ρ with a known probability distribution f_ρ, and the tag ranges are independent of the tag ID waveforms.

In particular, we model all tag waveforms as random impulse responses from a wide-sense-stationary, uncorrelated-scattering (WSSUS) fading channel with known bandwidth and scattering function. A brief discussion of the properties of such channels and the notation used to describe them in this document is given in the Appendix.

Under these assumptions, we derive the expression for the output signal-to-noise ratio (SNR) for an arbitrary combination of transmitted interrogation signal and linear receiver filter. Based on this expression, we derive an optimal interrogator configuration (i.e., transmitted signal/receiver filter combination) in the two extreme noise/interference regimes, i.e., noise-limited and interference-limited, under the additional assumption that the coherence bandwidth of the tags is much smaller than the total tag bandwidth. It should be noted that the assumption that the impulse response of the tag of interest is known precisely implies that the temperature and range of the tag are also known precisely, which is generally not the case in practice. However, analyzing interrogator performance under this simplifying assumption is much more straightforward and still provides a great deal of insight into the nature of the problem.

4.1. Basic Approach

Let $e^{-i2\pi f\tau_0}H_0(f)$ represent the known frequency response function (i.e., the Fourier transform of the impulse response) of the tag of interest, where τ_0 represents the known delay, if any, built into the tag response in order allow environmental clutter energy at the receiver to dissipate prior to when the true tag response is received. Similarly, let $e^{-i2\pi f\tau_k}H_k(f)$ for $k = 1, 2, \ldots, K$, represent the unknown frequency response functions of the K interfering tags.

[1] Note that referring to the clutter as interfering "tags" does not result in any loss of generality under the assumed model. That is, the interference may not be caused by other SAW RFID tags but rather by arbitrary reflected clutter.

If an arbitrary interrogating signal with frequency spectrum $H_T(f)$ and energy $\mathcal{E}$ is transmitted from the transmitting antenna, then the return signal from tag $k = 0, 1, \ldots, K,$ received at the (co-located) receiving antenna is given by

$$X_k(f) = \sqrt{\frac{\mathcal{E}}{\int_{-B/2}^{B/2} \left|H_T(f)\right|^2 df}} \cdot r_k^{-\alpha} H_T(f) H_k(f) e^{-i4\pi f(t_k/2 + r_k/c)},$$

where c is the signal propagation velocity and r_k is the range of the tag from both the transmitting and receiving antennas measured in meters.[2] If the receiver implements a filter with frequency response $H_R(f)$ sampled at output time $t = 0$, then the output from the receiver due only to the return signal $X_k(f)$ will be

$$S_k = \mathcal{E} r_k^{-\alpha} \int_{-B/2}^{B/2} H_R(f) \frac{H_T(f)}{\sqrt{\mathcal{E}_T}} H_k(f) e^{-i4\pi f(t_k/2 + r_k/c)} df,$$

where $\mathcal{E}_T = \int_{-B/2}^{B/2} \left|H_T(f)\right|^2 df$ and

$$H_R(f) = 0, \quad \forall \left|f\right| > B/2,$$

where B is the two-sided bandwidth of the filter.

Hence, the output from the receiver filter due to the signal of interest is given by

$$S_0 = \mathcal{E} r_0^{-\alpha} \int_{-B/2}^{B/2} H_R(f) \frac{H_T(f)}{\sqrt{\mathcal{E}_T}} H_0(f) e^{-i4\pi f(\tau_0/2 + r_0/c)} df,$$

and the aggregate interference from all of the interfering tags at the output of the receiver, is given by

$$\begin{aligned} I &= \sum_{k=1}^{K} S_k \\ &= \mathcal{E} \sum_{k=1}^{K} r_k^{-\alpha} \int_{-B/2}^{B/2} H_R(f) \frac{H_T(f)}{\sqrt{\mathcal{E}_T}} H_k(f) e^{-i4\pi f r_k/c} df \\ &= \mathcal{E} \int_{-B/2}^{B/2} H_R(f) \frac{H_T(f)}{\sqrt{\mathcal{E}_T}} \left[\sum_{k=1}^{K} r_k^{-\alpha} e^{-i4\pi f r_k/c} H_k(f) \right] df. \end{aligned}$$

Note that the aggregate interference represents a random variable with mean zero and variance

[2] Note that in this equation, all antenna gains are absorbed into the tag frequency response, and the amplitude decay rate for the return signal is $r^{-\alpha}$ rather than $r^{-\alpha/2}$ since this is a two-way or *cooperative radar* channel.

$$\sigma_I^2 = \int_{-B/2}^{B/2}\int_{-B/2}^{B/2} H_R(f)\frac{H_T(f)}{\sqrt{\mathcal{E}_T}}\bar{H}_R(\lambda)\frac{\bar{H}_T(\lambda)}{\sqrt{\mathcal{E}_T}}$$
$$\cdot\left[\sum_{k=1}^{K}\sum_{j=1}^{K}\mathrm{E}\left\{r_k^{-\alpha}r_j^{-\alpha}e^{-i4\pi f r_k/c}e^{i4\pi\lambda r_j/c}\right\}\mathrm{E}\left\{H_k(f)\bar{H}_j(\lambda)\right\}\right]dfd\lambda$$
$$= \mathcal{E}\int_{-B/2}^{B/2}\int_{-B/2}^{B/2} H_R(f)\frac{H_T(f)}{\sqrt{\mathcal{E}_T}}\bar{H}_R(\lambda)\frac{\bar{H}_T(\lambda)}{\sqrt{\mathcal{E}_T}}$$
$$\cdot\varphi(f-\lambda)\left[\sum_{k=1}^{K}\mathrm{E}\left\{r_k^{-2\alpha}e^{-i4\pi(f-\lambda)r_k/c}\right\}\right]dfd\lambda$$
$$= K\mathcal{E}\int_{-B/2}^{B/2}\int_{-B/2}^{B/2} H_R(f)\frac{H_T(f)}{\sqrt{\mathcal{E}_T}}\bar{H}_R(\lambda)\frac{\bar{H}_T(\lambda)}{\sqrt{\mathcal{E}_T}}\varphi(f-\lambda)\rho(f-\lambda)dfd\lambda,$$

where $\varphi_k(f-\lambda)\equiv\varphi(f-\lambda)$ is the *spaced-frequency correlation function* (see Appendix) for the interfering tags, and

$$\rho(f-\lambda) = \mathrm{E}\left\{\rho^{-2\alpha}e^{-i4\pi(f-\lambda)\rho/c}\right\}^{3}$$

represents a similar spaced-frequency correlation function for the multiplicative power decay and phase shift of the interfering tags.

Finally, the output from the receiver filter due to a complex-valued additive white Gaussian AWGN process with power spectral density N_0 and associated orthogonal increments frequency-domain process $Z(f)$ is given by

$$N = \int_{-B/2}^{B/2} H_R(f)Z(df),$$

which is a Gaussian random variable with mean zero and variance

$$\sigma_N^2 = N_0\int_{-B/2}^{B/2}\left|H_R(f)\right|^2 df\ .$$

Hence, if we let $Y = S_0 + I + N$ represent the random output from the receiver filter in the presence of the signal of interest, additive interference, and AWGN, then it follows that the output SNR at the receiver is given by

[3] Note that if all tags are at the same range $\rho = r_0$, then $\rho(f-\lambda) = r_0^{-2\alpha}e^{-i4\pi r_0/c}$.

$$SNR_{I+N} = \frac{\mathrm{E}\{Y\}}{\mathrm{Var}\{Y\}} = \frac{|S_0|^2}{\sigma_N^2 + \sigma_I^2}$$

$$= \frac{\mathcal{E} r_0^{-2\alpha} \left| \int_{-B/2}^{B/2} H_R(f) \frac{H_T(f)}{\sqrt{\mathcal{E}_T}} H_0(f) e^{-i4\pi f(\tau_0/2 + r_0/c)} df \right|^2}{K\mathcal{E} \int_{-B/2}^{B/2} \int_{-B/2}^{B/2} \left[H_R(f) \frac{H_T(f)}{\sqrt{\mathcal{E}_T}} \bar{H}_R(\lambda) \frac{\bar{H}_T(\lambda)}{\sqrt{\mathcal{E}_T}} \cdot \varphi(f-\lambda) \rho(f-\lambda) \right] df d\lambda + N_0 \int_{-B/2}^{B/2} |H_R(f)|^2 df}. \quad (5)$$

Assuming that the aggregate interference is well approximated as Gaussian, the detection performance of the interrogator is determined by this quantity. Such an assumption is probably only justified for a large number of interfering tags, but maximizing the output SNR remains a worthwhile optimization criterion in any case.

As a rule, Equation (5) can be simplified quite a bit by making the following additional assumptions, which should be valid approximately for tags with good anti-collision properties and appropriate choices of $H_T(f)$ and $H_R(f)$:

1. $\varphi(\upsilon) = 0 \; \forall |\upsilon| > \Delta/2$, where $\Delta << B$. Recall that Δ represents the *coherence bandwidth* for the set of tag waveforms,
2. $H_R(f) \approx H_R(\lambda), H_T(f) \approx H_T(\lambda) \; \forall |f - \lambda| < \Delta$,
3. $H_k(f) \approx H_k(\lambda) \; \forall |f - \lambda| < \Delta, k = 0, 1, \ldots, K$.

Under these assumptions, the expression for the variance becomes

$$\sigma_I^2 \approx K\mathcal{E} \int_{-B/2}^{B/2} \left| H_R(\lambda) \frac{H_T(\lambda)}{\sqrt{\mathcal{E}_T}} \right|^2 \int_{\lambda-\Delta/2}^{\lambda+\Delta/2} \varphi(f-\lambda) \rho(f-\lambda) df d\lambda$$

$$= K\mathcal{E} \int_{-B/2}^{B/2} \left| H_R(\lambda) \frac{H_T(\lambda)}{\sqrt{\mathcal{E}_T}} \right|^2 d\lambda \cdot \int_{-\Delta/2}^{\Delta/2} \varphi(\upsilon) \rho(\upsilon) d\upsilon,$$

which is a considerable simplification, and the expression for the output SNR becomes

$$SNR_{I+N} \approx \frac{\mathcal{E} r_0^{-2\alpha} \left| \int_{-B/2}^{B/2} H_R(f) \frac{H_T(f)}{\sqrt{\mathcal{E}_T}} H_0(f) e^{-i4\pi f(\tau_0/2 + r_0/c)} df \right|^2}{K\mathcal{E} \int_{-B/2}^{B/2} \left| H_R(f) \frac{H_T(f)}{\sqrt{\mathcal{E}_T}} \right|^2 df \cdot \int_{-\Delta/2}^{\Delta/2} \varphi(\upsilon)\rho(\upsilon) d\upsilon + N_0 \int_{-B/2}^{B/2} \left| H_R(f) \right|^2 df}$$

$$= \frac{\mathcal{E} r_0^{-2\alpha} \left| \int_{-B/2}^{B/2} H_R(f) \frac{H_T(f)}{\sqrt{\mathcal{E}_T}} H_0(f) e^{-i4\pi f(\tau_0/2 + r_0/c)} df \right|^2}{K\mathcal{E} N_I \int_{-B/2}^{B/2} \left| H_R(f) \frac{H_T(f)}{\sqrt{\mathcal{E}_T}} \right|^2 df + N_0 \int_{-B/2}^{B/2} \left| H_R(f) \right|^2 df},$$

where $N_I = \int_{-\Delta/2}^{\Delta/2} \varphi(\upsilon)\rho(\upsilon) d\upsilon$. Note that as $K\mathcal{E}N_I / N_0 \to \infty$, the interference term in the denominator dominates, and this expression simplifies to

$$SNR_I = \frac{r_0^{-2\alpha}}{KN_I} \cdot \frac{\left| \int_{-B/2}^{B/2} H_R(f) H_T(f) H_0(f) e^{-i4\pi f(\tau_0/2 + r_0/c)} df \right|^2}{\int_{-B/2}^{B/2} \left| H_R(f) H_T(f) \right|^2 df}. \tag{6}$$

On the other hand, as $K\mathcal{E}N_I / N_0 \to 0$, the AWGN term dominates, and the expression simplifies to

$$SNR_N = r_0^{-2\alpha} \frac{\mathcal{E}}{N_0} \cdot \frac{\left| \int_{-B/2}^{B/2} H_R(f) \frac{H_T(f)}{\sqrt{\mathcal{E}_T}} H_0(f) e^{-i4\pi f(\tau_0/2 + r_0/c)} df \right|^2}{\int_{-B/2}^{B/2} \left| H_R(f) \right|^2 df}. \tag{7}$$

4.2. Optimal Interrogation

Note that in the general case, the choice of the transmitted signal $H_T(f)$ and the receiver filter $H_R(f)$ that maximize the output SNR given by Expression (5) must be determined numerically by solving a fairly complex variational problem. Hence, in general, the optimal interrogator design and the corresponding detection performance is rather difficult to determine. However, for practical purposes, the problem can often be reduced to either the interference-limited case or the noise-limited case[4] given by Equations (6) and (7). In each of the two limiting cases, the optimal interrogator design and corresponding optimal output SNR are easy to determine. We consider each case separately below.

4.2.1. Noise-Limited Case

For this case, the output SNR is given by Expression (7) and satisfies

[4] The problem reduces to the interference-limited case as the product of the number of interfering tags and the energy of the transmitted signal goes to infinity. As the same product goes to zero, the problem reduces to the noise-limited case.

$$SNR_N = r_0^{-2\alpha}\frac{\mathcal{E}}{N_0}\cdot\frac{\left|\int_{-B/2}^{B/2} H_R(f)\frac{H_T(f)}{\sqrt{\mathcal{E}_T}}H_0(f)e^{-i4\pi f(\tau_0/2+r_0/c)}df\right|^2}{\int_{-B/2}^{B/2}\left|H_R(f)\right|^2 df}$$

$$\le r_0^{-2\alpha}\frac{\mathcal{E}}{N_0}\cdot\int_{-B/2}^{B/2}\left|\frac{H_T(f)}{\sqrt{\mathcal{E}_T}}H_0(f)\right|^2 df.$$

It follows from the Cauchy-Schwarz (C-S) inequality that equality is achieved in this expression if and only if

$$H_R(f) = \beta\frac{\bar{H}_T(f)}{\sqrt{\mathcal{E}_T}}\bar{H}_0(f)e^{i4\pi f(\tau_0/2+r_0/c)},$$

for an arbitrary complex constant $\beta \neq 0$. Furthermore, in this case (assuming that $H_0(f)$ is bounded on $f \in [-B/2, B/2]$ with $M_0 = \max_{f\in[-B/2,B/2]}\left|H_0(f)\right|$), we have

$$SNR_N = r_0^{-2\alpha}\frac{\mathcal{E}}{N_0}\cdot\int_{-B/2}^{B/2}\left|\frac{H_T(f)}{\sqrt{\mathcal{E}_T}}H_0(f)\right|^2 df \le r_0^{-2\alpha}\frac{\mathcal{E}}{N_0}M_0^2,$$

where equality is achieved if and only if

$$H_T(f) = \begin{cases}\text{arbitrary}, & H_0(f) = M_0,\\ 0, & H_0(f) \neq M_0,\end{cases}$$

such that $\int_{\{|H_0(f)|=M_0\}}\left|H_T(f)\right|^2 df \neq 0$. Unfortunately, this is not a very satisfying solution for several reasons. First, in many cases, i.e., when the set $\left\{\left|H_0(f)\right| = M_0\right\}$ consists of a single point or in general a set of measure zero, an optimal solution will not actually exist. In this case, the optimal solution can be approximated arbitrarily well by a solution for which $H_T(f)$ is non-zero on a set of positive measure, but as that set approaches the set $\left\{\left|H_0(f)\right| = M_0\right\}$, the transmitted solution will approach a simple sinusoid of arbitrarily long duration. Even in the case where $\left\{\left|H_0(f)\right| = M_0\right\}$ has positive measure and a true optimal solution does exist, the transmitted function will frequently be non-zero only over a very small bandwidth and therefore will have a very long duration, which is an undesirable result for reading RFID tags with a very short response duration. In addition, any desirable anti-collision and temperature sensing properties of the tag response will largely be nullified by such an interrogating signal.

Hence, if we insist on defining the optimal solution as the one that maximizes the output SNR subject to an energy constraint (which is what we have been doing), then our transmitted waveform will not have desirable properties. To rectify this situation, we look instead for signals

that maximize the output SNR subject to a constraint on the frequency localization, which implies an energy constraint as well. In particular, we wish to choose $H_T(f)$ to maximize

$$SNR_N = r_0^{-2\alpha} \frac{\mathcal{E}}{N_0} \cdot \int_{-B/2}^{B/2} \left| \frac{H_T(f)}{\sqrt{\mathcal{E}_T}} H_0(f) \right|^2 df$$

subject to the constraint

$$\mathcal{L}_{H_T} = \int_{-B/2}^{B/2} \left| H_T(f) \right|^4 df \le \mathcal{L}_{\max},$$

for some *frequency localization constraint* $\mathcal{L}_{\max}$ [5]. It follows that

$$\begin{aligned} r_0^{-2\alpha} \frac{\mathcal{E}}{N_0} \cdot \int_{-B/2}^{B/2} \left| \frac{H_T(f)}{\sqrt{\mathcal{E}_T}} H_0(f) \right|^2 df &= r_0^{-2\alpha} \frac{\mathcal{E}}{\mathcal{E}_T N_0} \cdot \int_{-B/2}^{B/2} \left| H_T(f) \right|^2 \left| H_0(f) \right|^2 df \\ &\le r_0^{-2\alpha} \frac{\mathcal{E}}{\mathcal{E}_T N_0} \cdot \sqrt{\int_{-B/2}^{B/2} \left| H_T(f) \right|^4 df} \cdot \sqrt{\int_{-B/2}^{B/2} \left| H_0(f) \right|^4 df} \\ &= r_0^{-2\alpha} \frac{\mathcal{E}}{\mathcal{E}_T N_0} \sqrt{\mathcal{L}_{H_T}} \cdot \sqrt{\int_{-B/2}^{B/2} \left| H_0(f) \right|^4 df} \\ &\le r_0^{-2\alpha} \frac{\mathcal{E}}{\mathcal{E}_T N_0} \sqrt{\mathcal{L}_{\max}} \cdot \sqrt{\int_{-B/2}^{B/2} \left| H_0(f) \right|^4 df}, \end{aligned}$$

with equality if and only if $\mathcal{L}_{H_T} = \mathcal{L}_{\max}$ and $\left| H_T(f) \right| = \gamma \left| H_0(f) \right|$ for some $\gamma \neq 0$. In particular, equality is achieved by choosing $H_T(f) = \gamma \bar{H}_0(f)$, which corresponds to transmitting the time-reverse of the impulse response of the tag of interest. It should be noted that this particular choice for the transmitted signal also produces a received signal with maximum peak power subject to an energy constraint. These and other properties of *time-reversal processing* are discussed in more detail in [Barton, et al.].

Hence, without loss of generality, the optimal frequency-localized interrogating signal satisfies

$$H_T(f) = \bar{H}_0(f),$$

the optimal receiver filter satisfies

$$H_R(f) = \beta \frac{\left| H_0(f) \right|^2}{\sqrt{\mathcal{E}_0}} e^{i4\pi f(\tau_0/2 + r_0/c)},$$

where $\mathcal{E}_0 = \int_{-B/2}^{B/2} \left| H_0(f) \right|^2 df$ and $\beta \neq 0$ is arbitrary, and the optimal output SNR is given by

[5] For a discussion of the physical intuition motivating this constraint, the interested reader is referred to [Barton and Zheng].

$$SNR_N^* = r_0^{-2\alpha} \frac{\mathcal{E}}{\mathcal{E}_0 N_0} \cdot \int_{-B/2}^{B/2} \left| H_0(f) \right|^4 df \, .$$

Finally, averaging over the constellation of random tag waveforms gives

$$\overline{SNR}_N^* = r_0^{-2\alpha} \frac{\mathcal{E}}{N_0} \cdot \mathrm{E}\left\{ \frac{1}{\mathcal{E}_0} \int_{-B/2}^{B/2} \left| H_0(f) \right|^4 df \right\}.$$

4.2.2. Interference-Limited Case

For this case, the output SNR is given by Expression (6) and satisfies

$$SNR_I = \frac{r_0^{-2\alpha}}{KN_I} \cdot \frac{\left| \int_{-B/2}^{B/2} H_R(f) H_T(f) H_0(f) e^{-i4\pi f(\tau_0/2 + r_0/c)} df \right|^2}{\int_{-B/2}^{B/2} \left| H_R(f) H_T(f) \right|^2 df} \le \frac{r_0^{-2\alpha}}{KN_I} \int_{-B/2}^{B/2} \left| H_0(f) \right|^2 df \, .$$

Again, it follows from the C-S inequality that equality is achieved in this expression if and only if

$$H_R(f) H_T(f) = \beta \bar{H}_0(f) e^{i4\pi f(\tau_0/2 + r_0/c)},$$

for an arbitrary complex constant $\beta \neq 0$. Hence, one possible choice for the optimal interrogating signal satisfies

$$H_T(f) = \begin{cases} 1, & |f| \le B/2, \\ 0, & |f| > B/2, \end{cases}$$

the corresponding optimal receiver filter satisfies

$$H_R(f) = \beta \bar{H}_0(f) e^{i4\pi f(\tau_0/2 + r_0/c)},$$

where $\beta \neq 0$ is arbitrary, and the optimal output SNR is given by

$$SNR_I^* = \frac{r_0^{-2\alpha}}{KN_I} \int_{-B/2}^{B/2} \left| H_0(f) \right|^2 df \, .$$

Finally, averaging over the constellation of random tag waveforms gives

$$\overline{SNR}_I^* = \frac{r_0^{-2\alpha}}{KN_I} \mathrm{E}\left\{ \int_{-B/2}^{B/2} \left| H_0(f) \right|^2 df \right\} = \frac{r_0^{-2\alpha}}{KN_I} B \varphi_0(0),$$

where $\varphi_0(\upsilon)$ is the spaced-frequency correlation function for the tag of interest.

Notice that in this case, the optimal transmitted signal is just a band-limited impulse function, which can be approximated using either a stepped CW signal or an FM chirp.

5. Interrogator Performance Evaluations

To compare the performance of the two interrogator configurations derived in Sections 4.2.1 and 4.2.2 above (which would be optimal in the noise-limited case and the interference-limited case, respectively, if all of our assumptions were satisfied), and to determine whether our assumed

WSSUS model for tag waveforms is really useful as a basis for performance predictions, we computed the value of the output SNR for each configuration both numerically and using Monte Carlo simulation over a range of operational scenarios. Both the numerical computations and the simulations were based on a large constellation of simulated SAW tag waveforms that were generated using a tag-design algorithm under investigation at NASA JSC. Whether or not these simulated waveforms are reasonable approximations of tags that can actually be physically implemented remains to be seen, but at least this approach provides a very large set of known tag waveforms that can be used to generate statistics for numerical computations and as a basis for Monte Carlo simulations to validate the numerical computations.

All performance results were derived from a collection of 4096 simulated tag frequency-response vectors that were generated randomly in an iid fashion. All simulated tags had a center frequency of $f_0 = 2.44$ GHz, a useable bandwidth of approximately $B = 80$ MHz, and a duration of $T = 2.6$ μs. Hence, the time-bandwidth product for the tag constellation was $BT = 208$ and the bit-rate was $R = 12$ bits per tag. Numerical performance results were derived by evaluating Equation (5) numerically using a sampled version of $\varphi(f - \lambda)$ estimated directly from the population of tag frequency response vectors. Simulated performance was derived by generating random realizations of the random variable $Y = S_0 + I + N$ that underlies Equation (5) , directly estimating the quantities $\mathrm{E}\{Y\}$ and $\mathrm{Var}\{Y\}$, and computing an estimate of output SNR as $\mathrm{E}\{Y\}/\mathrm{Var}\{Y\}$. Note that for all of these performance results presented in this section, the tag center frequency and the tag bit-rate corresponding to the chosen constellation size are actually irrelevant, since neither parameter appears in the interrogator performance results derived in Section 4. Hence, these particular performance evaluations shed no light on the collision resolution characteristics of the simulated tags relative to the theoretical bounds derived in Section 3. Studies along those lines are planned for the future when more is understood about generation of realistic simulated tag waveforms. Nevertheless, both the output SNR and its rate of change with respect to number of tags in the environment are quite useful for comparing the relative collision-resolution behavior of different interrogator designs.

For the performance results presented in this section, all tags (i.e., the tag of interest as well as all interfering tags) were assumed to be at the same range, represented by the variable R_0, propagation was assumed to be in free space (i.e., $\alpha = 2$), the antenna temperature was assumed to be $T_0 = 300°$ Kelvin, the transmit power from the interrogator was set to $P_T = 1 \times 10^{-2}$ Watts (10 mw) and the integration (dwell) time at the receiver was set to $D_T = 2.5 \times 10^{-2}$ sec (25 ms). The assumed gain of the interrogator is represented by the variable G_T, the gain of the tag antenna is represented by the variable G_R, and all tag frequency-response waveforms were scaled to correspond to an insertion loss of approximately $L_i = 1 \times 10^{-3}$ (30 dB) in total tag input vs. output energy. Letting $K_B = 1.38 \times 10^{-12}$ represent Boltzman's constant, it follows that in Equation (5), the total transmitted energy is given by $\mathcal{E} = P_T D_T G_T^2 G_R^2 L_i$ and the noise power spectral density is given by $N_0 = K_B T_0$. It also follows that for all figures, the output SNR value for the interference-optimal (i.e., band-limited impulse) interrogator with no interfering tags corresponds exactly to the value of SNR at the input to the receiver (i.e., $\mathcal{E}_s / N_0$) computed using a traditional link-budget calculation.

Note that for the noise-optimal interrogator, Equation (5) reduces to

$$SNR_{I+N} = \frac{\frac{\mathcal{E}}{\mathcal{E}_0^2} r_0^{-2\alpha} \left| \int_{-B/2}^{B/2} \left| H_0(f) \right|^4 \right|^2}{\frac{K\mathcal{E}}{\mathcal{E}_0^2} \int_{-B/2}^{B/2} \int_{-B/2}^{B/2} \left[\begin{array}{l} \left| H_0(f) \right|^2 \left| H_0(\lambda) \right|^2 \bar{H}_0(f) H_0(\lambda) \\ \cdot e^{i4\pi(f-\lambda)(\tau_0/2 + r_0/c)} \varphi(f-\lambda) \rho(f-\lambda) \end{array} \right] df d\lambda + \frac{N_0}{\mathcal{E}_0} \int_{-B/2}^{B/2} \left| H_0(f) \right|^4 df}, \quad (8)$$

while for the interference-optimal interrogator, it reduces to

$$SNR_{I+N} = \frac{\frac{\mathcal{E}}{B} r_0^{-2\alpha} \left| \int_{-B/2}^{B/2} \left| H_0(f) \right|^2 df \right|^2}{\frac{K\mathcal{E}}{B} \int_{-B/2}^{B/2} \int_{-B/2}^{B/2} \left[\begin{array}{l} \bar{H}_0(f) H_0(\lambda) e^{i4\pi(f-\lambda)(\tau_0/2 + r_0/c)} \\ \cdot \varphi(f-\lambda) \rho(f-\lambda) \end{array} \right] df d\lambda + N_0 \int_{-B/2}^{B/2} \left| H_0(f) \right|^2 df}. \quad (9)$$

As it turns out, although both of these equations give reasonable predictions of interrogator performance, considerably better predictions can be obtained by eliminating the assumption that the frequency-domain correlation function φ for the random tag frequency response function is stationary. That is, we replace the function $\varphi(f-\lambda)$ by the more general function $\varphi(f,\lambda)$, which is equivalent to using a wide-sense stationary, but *correlated* scattering model rather than the standard WSSUS model. In this case, Equations (8) and (9) become

$$SNR_{I+N} = \frac{\frac{\mathcal{E}}{\mathcal{E}_0^2} r_0^{-2\alpha} \left| \int_{-B/2}^{B/2} \left| H_0(f) \right|^4 \right|^2}{\frac{K\mathcal{E}}{\mathcal{E}_0^2} \int_{-B/2}^{B/2} \int_{-B/2}^{B/2} \left[\begin{array}{l} \left| H_0(f) \right|^2 \left| H_0(\lambda) \right|^2 \bar{H}_0(f) H_0(\lambda) \\ \cdot e^{i4\pi(f-\lambda)(\tau_0/2 + r_0/c)} \varphi(f,\lambda) \rho(f-\lambda) \end{array} \right] df d\lambda + \frac{N_0}{\mathcal{E}_0} \int_{-B/2}^{B/2} \left| H_0(f) \right|^4 df}, \quad (10)$$

and

$$SNR_{I+N} = \frac{\frac{\mathcal{E}}{B} r_0^{-2\alpha} \left| \int_{-B/2}^{B/2} \left| H_0(f) \right|^2 df \right|^2}{\frac{K\mathcal{E}}{B} \int_{-B/2}^{B/2} \int_{-B/2}^{B/2} \left[\begin{array}{l} \bar{H}_0(f) H_0(\lambda) e^{i4\pi(f-\lambda)(\tau_0/2 + r_0/c)} \\ \cdot \varphi(f,\lambda) \rho(f-\lambda) \end{array} \right] df d\lambda + N_0 \int_{-B/2}^{B/2} \left| H_0(f) \right|^2 df}. \quad (11)$$

Equations (10) and (11) were used to generate the numerical performance results in the remainder of this section.

Figures 4-8 illustrate the results of the performance evaluation for the two interrogators with 3 dB-gain antennas on each end of the link. Each figure corresponds to the performance at a particular assumed range for all responding tags in the environment, and the plots displayed in each figure represent the output SNR for each of the two interrogators of interest as a function of the number of responding tags over the range 1-25 tags. There are a total of four curves plotted in each figure: a numerical estimate of the output SNR curve for each interrogator and a simulated output SNR curve for each. In each case, the simulated results agree very closely with the numerical results, which validates the analytical model of tag behavior developed in this paper, at least for the constellation of simulated tag waveforms studied here. The implication is

that a quantity of significant interest for evaluating the collision resolution behavior for a particular tag constellation is the non-stationary version of the frequency-domain correlation function $\varphi(f,\lambda)$ for the tag frequency-response functions $H(f)$.

There are several features of interest in the plots displayed in Figures 4-8. First, as discussed earlier, the maximum value of the red (and blue) curve in each plot represents the value of the SNR associated with a typical link budget calculation for a single tag in the environment. As expected, this value falls off at a rate of R_0^{-4} as the range increases, and as a general rule, acceptable performance for any number of tags can only be expected if this value exceeds approximately 12 dB (confer [Proakis, Figure 5.2-4]). Hence, for this configuration, tags could only be read reliably to a range of slightly more than 20 meters. Second, for a single tag in the environment, which corresponds to the noise-limited operating regime, the noise-optimal interrogator always outperforms the interference-optimal interrogator, as it should. The cross-over point of the red/blue and green/teal curves, at which the interference begins to dominate and the interference-optimal interrogator begins to outperform the noise-optimal interrogator, depends on range, but for short ranges, the interference begins to dominate with only two tags (i.e., a single interfering tag) in the environment. Finally, in the interference-limited operating region, i.e., well beyond the cross-over point of the interference- and noise-optimal curves, the performance of both interrogators is essentially independent of range (and therefore path-loss exponent α as well) and the asymptotic performance advantage of the interference-optimal interrogator is about 2 dB. The range independence is exactly as predicted by Equations (10) and (11), but the actual value of the asymptotic performance advantage of the interference-optimal interrogator depends on tag-response characteristics of the chosen tag constellation.

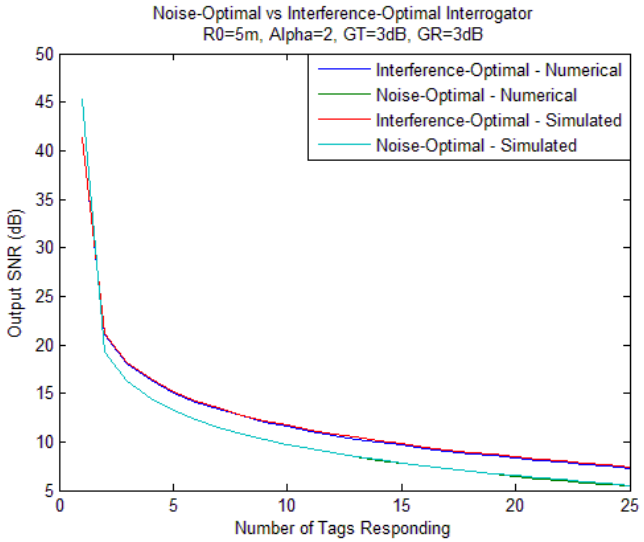

Figure 4. Interrogator Performance at range $R_0 = 5$ meters with antenna gains $G_T = G_R = 3$ dB.

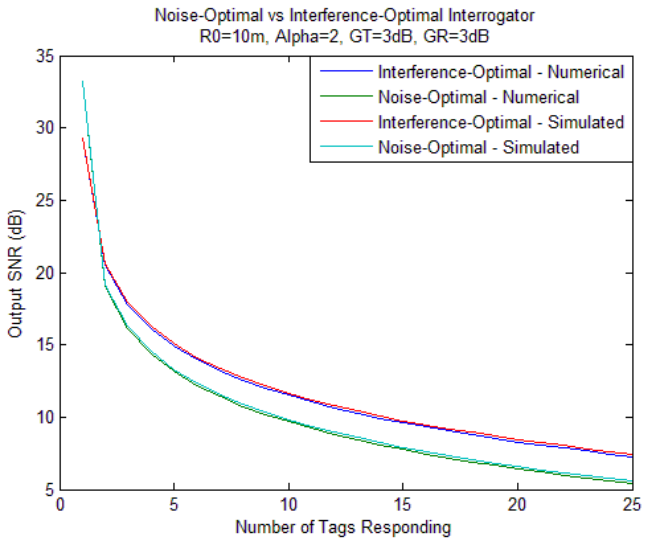

Figure 5. Interrogator Performance at range $R_0 = 10$ meters with antenna gains $G_T = G_R = 3$ dB.

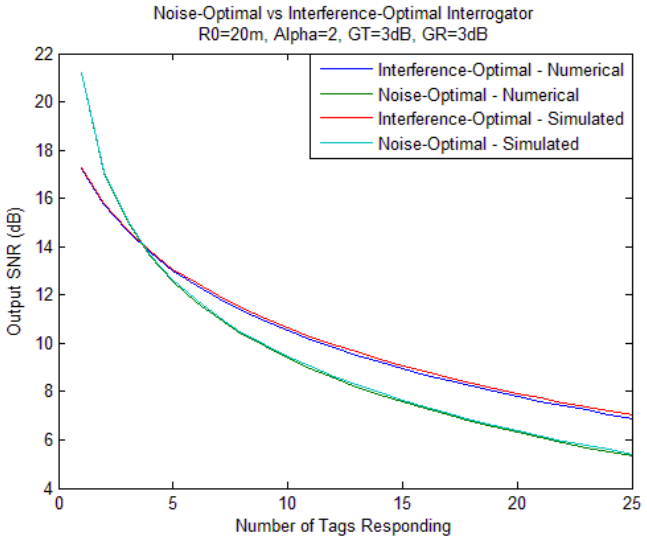

Figure 6. Interrogator Performance at range $R_0 = 20$ meters with antenna gains $G_T = G_R = 3$ dB.

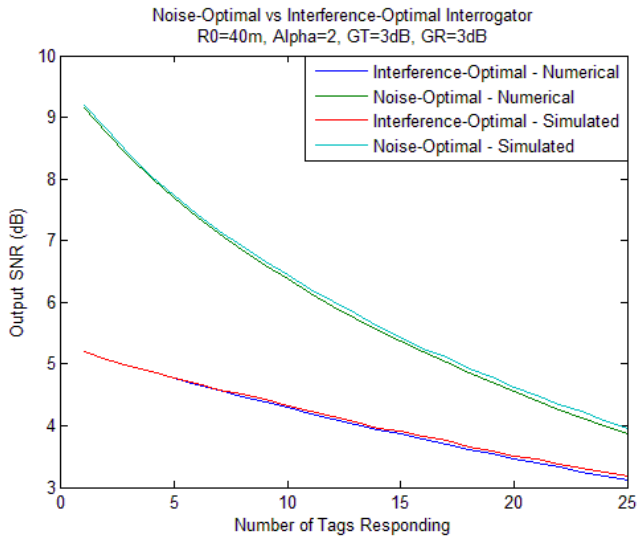

Figure 7. Interrogator Performance at range $R_0 = 40$ meters with antenna gains $G_T = G_R = 3$ dB.

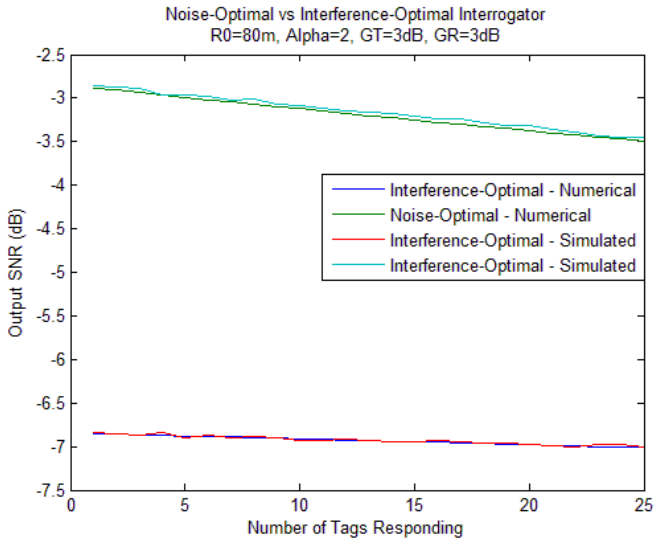

Figure 8. Interrogator Performance at range $R_0 = 80$ meters with antenna gains $G_T = G_R = 3$ dB.

For comparison purposes, a second set of performance curves was generated assuming an interrogator with a high-gain antenna with $G_T = 12$ dB. All other operating parameters remained the same. These results are illustrated in Figures 9-13. A couple of additional features of interest regarding interrogator performance can be gleaned from comparing the high-gain antenna results to the previous results. The first, which is quite obvious, is that system performance can be improved dramatically by adding antenna gain at the interrogator. The same would be true for additional gain in the tag antennas, but that is much more difficult to accomplish due to the size of the tags, the difficulty of knowing the exact orientation of all tag antennas, and the expense of adding a high-gain antenna to a large number of tags. In contrast, increasing the gain of the interrogator antenna does not unreasonably increase either the cost or size of the interrogator and

controlling the orientation of the interrogator is a simple matter. For the current configuration, increasing the interrogator antenna gain from 3 dB to 12 dB, which is fairly modest, increases the reliable read range from just over 20 meters to nearly 80 meters.

The second point of interest, which is less obvious, is that interrogator performance in the presence of both tag mutual interference and noise is not simply a function of the product of near-field SNR ($\mathcal{E}/N_0$) and path-loss factor (R_0^{-4}), as it would be in the presence of noise alone. That is, when interrogating multiple tags, the effects of range cannot be compensated for completely simply by increasing the gain of the system antennas. This can be seen quite clearly by noting that the performance of both interrogators in the interference-limited operating region is relatively insensitive to both range and antenna gain and also by studying the performance cross-over points for the noise-optimal versus interference-optimal interrogators in the two cases. In particular, with the low-gain interrogator antenna, for all ranges at which the single-tag link-budget SNR (maximum value on the red/blue curve) is large enough to provide reliable detection from some number of tags (i.e., above 12 dB), the performance is interference limited when there are more than two tags responding. Hence, there would be no advantage to using the noise-optimal interrogator with more than two tags in the environment. In contrast, with the high-gain interrogator antenna, reliable detection is still possible at nearly 80 meters but the performance at 80 meters becomes interference limited only when the number of tags responding exceeds 10. Hence, in this situation, there would be a distinct advantage to using the noise-optimal interrogator even with many tags in the environment.

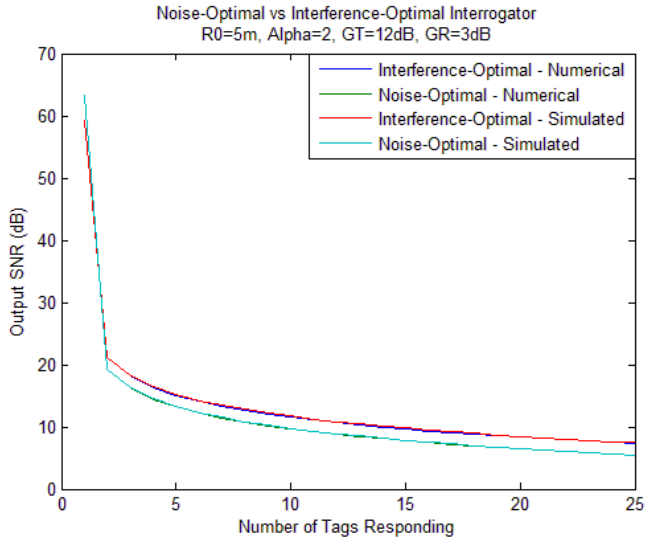

Figure 9. Interrogator Performance at range $R_0 = 5$ meters with antenna gains $G_T = 12$ dB and $G_R = 3$ dB.

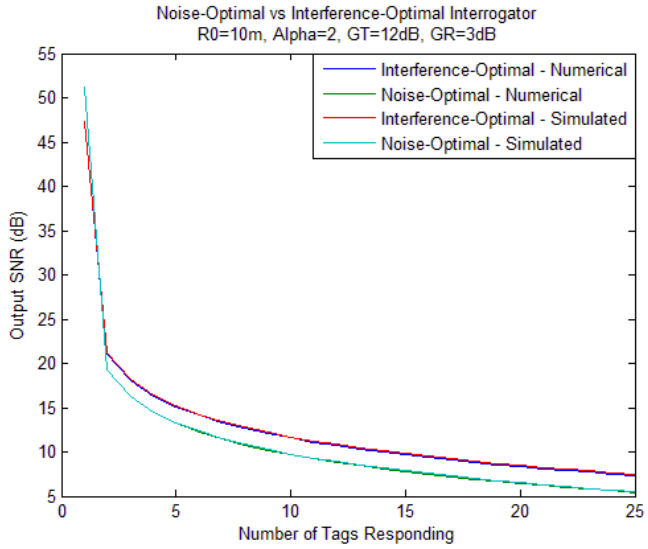

Figure 10. Interrogator Performance at range $R_0 = 10$ meters with antenna gains $G_T = 12$ dB and $G_R = 3$ dB.

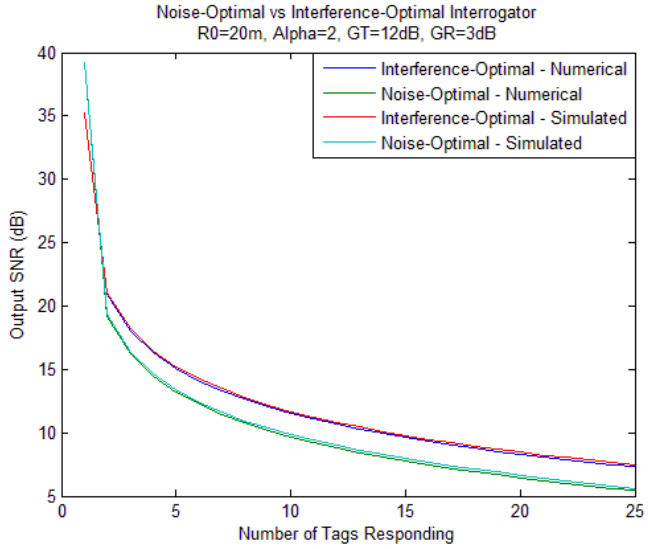

Figure 11. Interrogator Performance at range $R_0 = 20$ meters with antenna gains $G_T = 12$ dB and $G_R = 3$ dB.

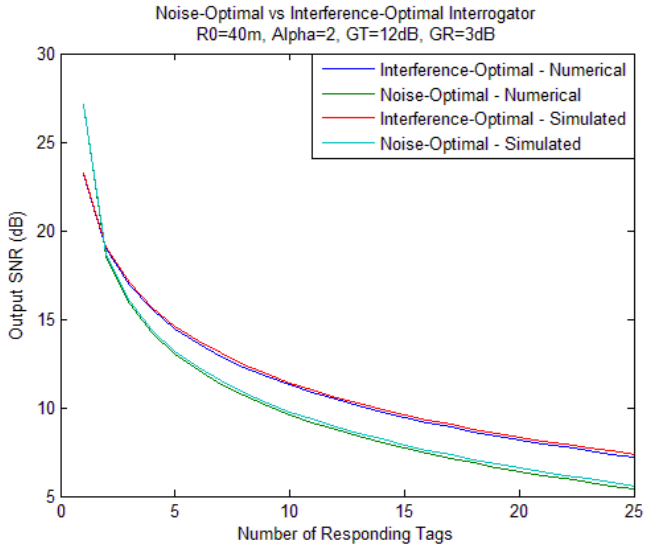

Figure 12. Interrogator Performance at range $R_0 = 40$ meters with antenna gains $G_T = 12$ dB and $G_R = 3$ dB.

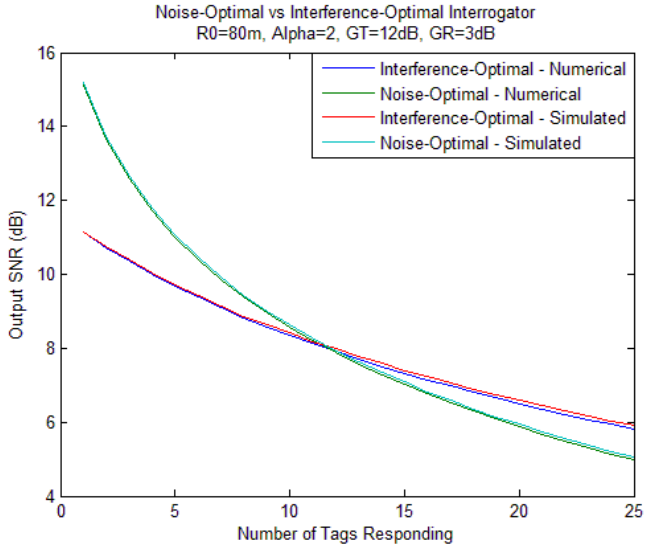

Figure 13. Interrogator Performance at range $R_0 = 80$ meters with antenna gains $G_T = 12$ dB and $G_R = 3$ dB.

6. Conclusion

In this paper, we have investigated several aspects of SAW interrogator design and performance. We first developed several theoretical results regarding the achievable data rates for SAW tags and discussed how these results relate to tag signal characteristics such as time-bandwidth product, SNR, and number of tags in the environment. In particular, we developed expressions for both an upper bound and a practical limit on the number of tags that can be jointly decoded for fixed values of SNR, time-bandwidth product, and achievable data rate. We also demonstrated that tags with good collision resolution properties can be expected to have waveforms with relatively long duration and low average power and that efficient use of the

channel (in terms of achievable data rate per tag per unit of SNR) can only be achieved if the time-bandwidth product of the tags greatly exceeds the product of SNR and the number of tags in the environment.

We then studied the problem of SAW interrogator design and developed an analytical expression for the output SNR of a linear interrogator reading a single known tag in the environment in the presence of both AWGN and interference from other tags in the environment based on a fairly general and realistic statistical model for tag frequency response. Subject to some further restrictions on this model, we also developed analytical expressions for the frequency response of optimal interrogators in both noise-limited and interference-limited environments. Based on these interrogator designs we developed expressions for the output SNR of both the interference-optimal and noise-optimal interrogators with respect to the original model as well as a slight relaxation of the original model that leads to better agreement with interrogator simulation studies.

Finally, interrogator performance was evaluated over a wide range of operating scenarios using both numerical evaluation of the analytical results developed in this paper as well as with Monte Carlo simulations. It was shown that the analytical results are very well supported by simulated interrogator performance, implying that predictions of interrogator performance can be made reliably using these analytical results. Further, it was demonstrated that interrogator performance is a fairly complicated function of range, near-field SNR, tag frequency correlation function, and number of tags in the environment. Hence, careful evaluation of predicted interrogator performance based on a range of environmental and configuration parameters can provide a great deal of insight into the which type of interrogator to use and what to expect in terms of achievable tag read range and collision resolution under practical scenarios.

References

Appendix. Background on Wide-Sense-Stationary Uncorrelated-Scattering Fading Channels

In this appendix, we review the basic concepts and notation for the wide-sense-stationary, uncorrelated-scattering (WSSUS) statistical model of multipath fading channels that is utilized in the previous sections of this document. For a much more thorough discussion, see, for example, [3].

We assume that the channel under consideration has a time-varying impulse response given by $h(\tau;t)$, where t represents the time at which the output is measured and τ represents the delay of the measurement. That is, $h(\tau;t)$ represents the output of the channel at time t due to an impulse transmitted at time $t-\tau$. It is further assumed that $h(\tau;t)$ is a zero-mean, complex random process that is causal, stationary in t, and satisfies the uncorrelated scattering assumption; *i.e.*,

$\mathrm{E}\{h(\tau;t)\} = 0 \;\forall t,\tau$,

and

$$\mathrm{E}\{h(\tau_1;t_1)\bar{h}(\tau_2;t_2)\} = \begin{cases} \hat{\varphi}(\tau_1;t_1-t_2)\delta(\tau_1-\tau_2), & \tau_1 \geq 0, \\ 0, & \text{otherwise,} \end{cases}$$

where an overbar indicates complex conjugation, and $\delta(\tau)$ represents the Dirac delta function. Note that if we want to avoid δ functions, we can express everything in the delay frequency domain. That is, if we define the Fourier transform of $h(\tau;t)$ with respect to τ as

$$H(f;t) = \int_{-\infty}^{\infty} h(\tau;t)e^{-i2\pi f\tau}d\tau,$$

then we get

$$\begin{aligned} \mathrm{E}\{H(f_1;t_1)\bar{H}(f_2;t_2)\} &= \int_0^{\infty}\int_0^{\infty} \mathrm{E}\{h(\tau_1;t_1)\bar{h}(\tau_2;t_2)\}e^{-i2\pi f_1\tau_1}e^{i2\pi f_2\tau_2}d\tau_1 d\tau_2 \\ &= \int_0^{\infty} \hat{\varphi}(\tau_1;t_1-t_2)e^{-i2\pi\tau_1(f_1-f_2)}d\tau_1 \\ &= \varphi(f_1-f_2;t_1-t_2), \end{aligned}$$

where φ represents the so-called *spaced-time, spaced-frequency correlation function*. Note that φ is only a function of the difference in both time and frequency; that is, the random process $H(f;t)$ is stationary in both variables. If the explicit output time is not of interest, the t is frequently dropped in favor of the short-hand notation $H(f)$. Similarly, when $t_1-t_2=0$, the notation $\varphi(f_1-f_2;0)$ is usually replaced by $\varphi(f_1-f_2)$, which is then referred to simply as the *spaced frequency correlation function.*

Note also that φ is often described in terms of its 2-D Fourier transform, which is given by

$$\mathcal{S}(\tau;\lambda) = \int_{-\infty}^{\infty}\int_{-\infty}^{\infty} \varphi(f;t)e^{i2\pi\tau f}e^{-i2\pi\lambda t}dfdt$$

The function $\mathcal{S}(\tau;\lambda)$ is generally referred to as the *scattering function* of the channel and represents the power spectral density of the two-dimensional stationary random process $H(f;t)$. Finally, it should be noted that we make the assumption of zero mean primarily for simplicity in exposition, but it is realistic in many cases, particularly if the channel has no line-of-sight component. In any case, extending the results to account for nonzero mean is straightforward.

Now, if we transmit a signal $s(t)$ over such a channel, then, ignoring additive noise, the output is a zero-mean, complex random process of the form

$$r(t) = \int_{-\infty}^{\infty} h(\tau;t)\, s(t-\tau)\, d\tau,$$

The autocorrelation function of this process is given by

$$\begin{aligned}
\mathrm{E}\{r(t_1)\overline{r}(t_2)\} &= \mathrm{E}\left\{\left[\int_{-\infty}^{\infty} h(\tau_1;t_1)\, s(t_1-\tau_1)\, d\tau_1\right]\left[\int_{-\infty}^{\infty} \overline{h}(\tau_2;t_2)\, \overline{s}(t_2-\tau_2)\, d\tau_2\right]\right\} \\
&= \int_{-\infty}^{\infty}\int_{-\infty}^{\infty} \mathrm{E}\{h(\tau_1;t_1)\overline{h}(\tau_2;t_2)\}\, s(t_1-\tau_1)\, \overline{s}(t_2-\tau_2)\, d\tau_1 d\tau_2 \\
&= \int_{-\infty}^{\infty} \hat{\varphi}(\tau_1;t_1-t_2)\, s(t_1-\tau_1)\, \overline{s}(t_2-\tau_1)\, d\tau_1,
\end{aligned}$$

Note that this autocorrelation function implies that the output is generally a nonstationary process unless the signal has some special properties. For example, if $s(t)$ is itself a zero mean, stationary random process that is independent of the channel process, then

$$\begin{aligned}
\mathrm{E}\{r(t_1)\overline{r}(t_2)\} &= \int_{-\infty}^{\infty} \hat{\varphi}(\tau_1;t_1-t_2)\, \mathrm{E}\{s(t_1-\tau_1)\, \overline{s}(t_2-\tau_1)\}\, d\tau_1 \\
&= \varphi_s(t_1-t_2)\cdot\left[\int_{-\infty}^{\infty} \hat{\varphi}(\tau_1;t_1-t_2)\, d\tau_1\right],
\end{aligned}$$

where $\varphi_s(t_1-t_2)$ represents the autocorrelation function of the signal.